

A late Carboniferous palaeomagnetic pole recorded from a syenite sill, Stabben, Central Norway

B.A. Sturt

Geological Survey of Norway, Leif Eirikssons vei 39, P.O. Box 3006, N-7001 Trondheim (Norway)

T.H. Torsvik

University of Bergen, Institute of Geophysics, N-5014 Bergen-University (Norway)

(Received January 19, 1987; revision accepted April 10, 1987)

Sturt, B.A. and Torsvik, T.H., 1987. A late carboniferous palaeomagnetic pole recorded from a syenite sill, Stabben, Central Norway. *Phys. Earth Planet. Inter.*, 49: 350–359.

High-blocking remanence components ($D = 192^\circ$, $I = -12^\circ$) recorded in a syenite sill from the Island of Stabben, Central Norway, are considered to be of primary/deuteric origin and to correspond to the radiometric age (297 Ma). The upper part of the sill and the contact gneiss, however, are strongly contaminated by a younger magnetic overprint ($D = 8^\circ$, $I = 59^\circ$). The primary component may represent a reliable Upper Carboniferous pole determination from Western Scandinavia, whereas the secondary component most probably relates to Cretaceous or younger faulting.

1. Introduction

In the Western Gneiss region, Central Norway (Fig. 1), the occurrence of post-Caledonian syenite porphyry dykes and sills has been described by Råheim (1974) on Tustna and indicated by Askvik and Rokoengen (1985) on Stabben (Fig. 1). From one of the dykes an age of 297 ± 8 Ma (Rb/Sr; whole-rock isochron) was obtained, apparently younger than the 370 Ma biotite age (K/Ar, $^{40}\text{Ar}/^{39}\text{Ar}$) obtained from a lamprophyre dyke at Ytterøy, north of Trondheim (Priem et al., 1968; Mitchell and Roberts, 1986).

According to Råheim (1974) the overall chemistry of the Tustna dyke shows gross similarities with the Permian igneous suite in the Oslo area, notably the Nordmarkite-ekerite series. The syenites on the island of Tustna and Stabben occur as subconcordant sheets which intrude a variety of gneissic rocks (Fig. 1). This account,

which is part of an ongoing project on the palaeomagnetism of mineralization zones and fault breccias in the Trondheimsfjord area, discusses the palaeomagnetic results from a vertical profile through a sill and its upper contact with gneiss, from the island of Stabben (lower contact not sampled as it was covered by high tide). A total of 22 orientated drill-cores (Samples 1–22) and two orientated hand-samples (Samples 23 and 214) were collected. The average vertical thickness of the sill is 2.45 m—preferred mineral lineations can be observed along the chilled margin (c. 3 cm) in the upper part of the sill.

2. Laboratory experiments

The anisotropy of magnetic susceptibility was studied by means of a low-induction susceptibility bridge (KLY-1), and the natural remanent magne-

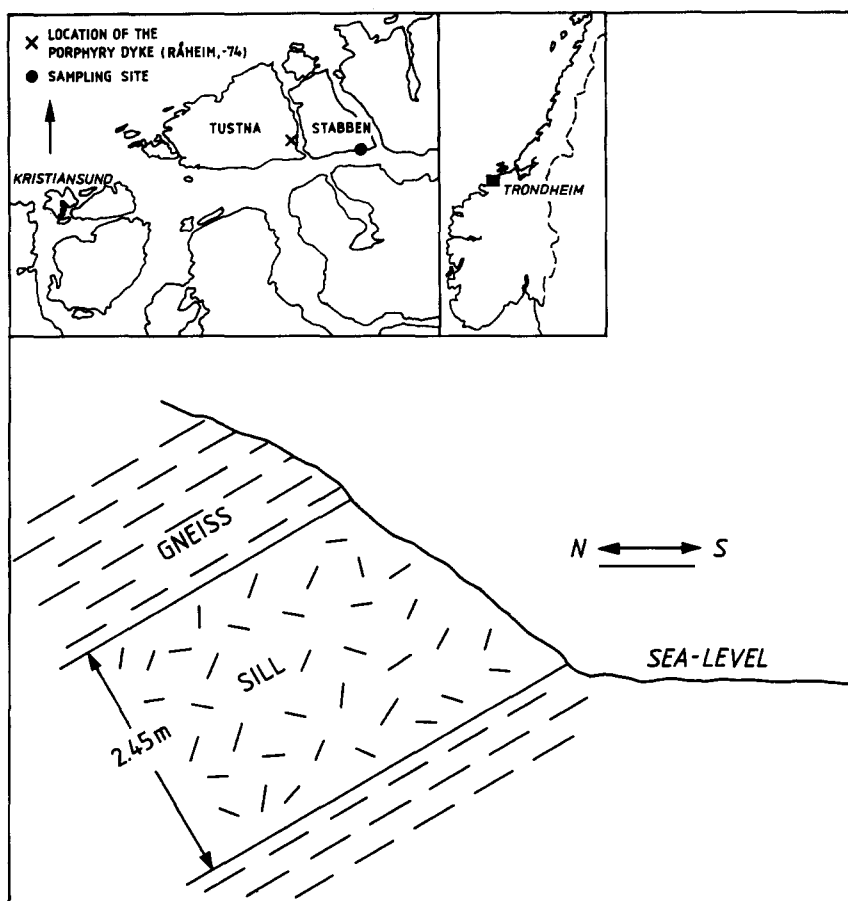


Fig. 1. Geographical location of the Stabben sill (simplified from Råheim (1974)) and a sketch of the sill and contact gneiss.

tization (NRM) was measured on a Molspin magnetometer. The stability of NRM was tested by stepwise thermal and to some extent alternating field (AF) demagnetization. Characteristic remanence components were obtained by least square line fitting in orthogonal vector-diagrams.

The concordant nature of the sill, with respect to the gneiss foliation (092/42N), is illustrated from the magnetic fabric data. Measurement of the anisotropy of magnetic susceptibility (Fig. 3) in the gneiss shows that the magnetic foliation ($K_{\max} - K_{\min}$) closely corresponds to the foliation, i.e. an intermediate inclined foliation with near E-W strike, and the shape of the magnetic ellipsoids are all oblate with total anisotropies around 8–12% (Fig. 2). Total anisotropy in the sill is lower, generally around 5%, and the magnetic

foliation is almost parallel to the gneissic foliation/sill margin. The central parts of the sill give oblate magnetic ellipsoids, whereas the upper and lower parts show well developed prolate ellipsoids. The magnetic fabric pattern in the sill is consistent with an original intrusive flow-fabric.

The NRM intensity in the contact gneiss (Fig. 2) is low (mean c. 0.5 mA m^{-1}): the upper part of the sill coincides with an increase in NRM intensity (to c. $10\text{--}15 \text{ mA m}^{-1}$), though a pronounced transition to a high intensity plateau can be recognized at c. 0.5 m below the upper contact (mean c. 60 mA m^{-1}). This intensity plateau corresponds to a strong increase of the Königberger ratio ($Q' = J_{\text{NRM}}/\text{Susceptibility}$).

The variations in NRM and Q' are closely related to the magnetic stability. The NRM direc-

tions from the gneiss and upper part of the sill are dominated by northerly and steeply downward pointing inclinations presumably of young origin (Fig. 4A,B); whereas the NRM of specimens from

the central and lower part of the sill define a southerly and almost sub-horizontal remanence group. Some gneiss specimens have a smeared distribution of southerly (Fig. 4A), but more

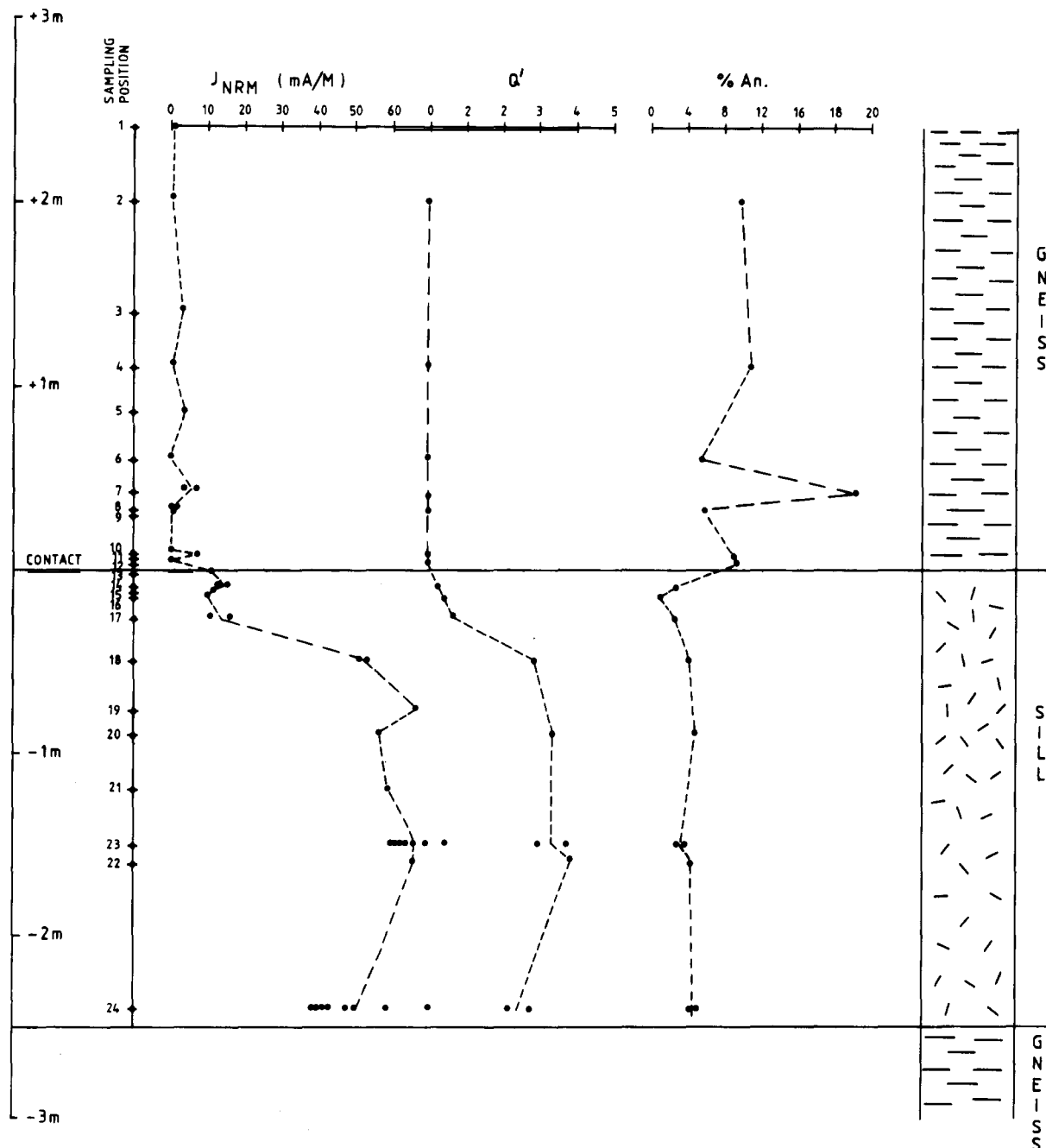


Fig. 2. Natural remanent magnetization (NRM), Königsberger ratio (Q') and degree of anisotropy (%An) through the sill and the upper gneiss contact. Sampling position (sample-names) shown to the left in the diagram.

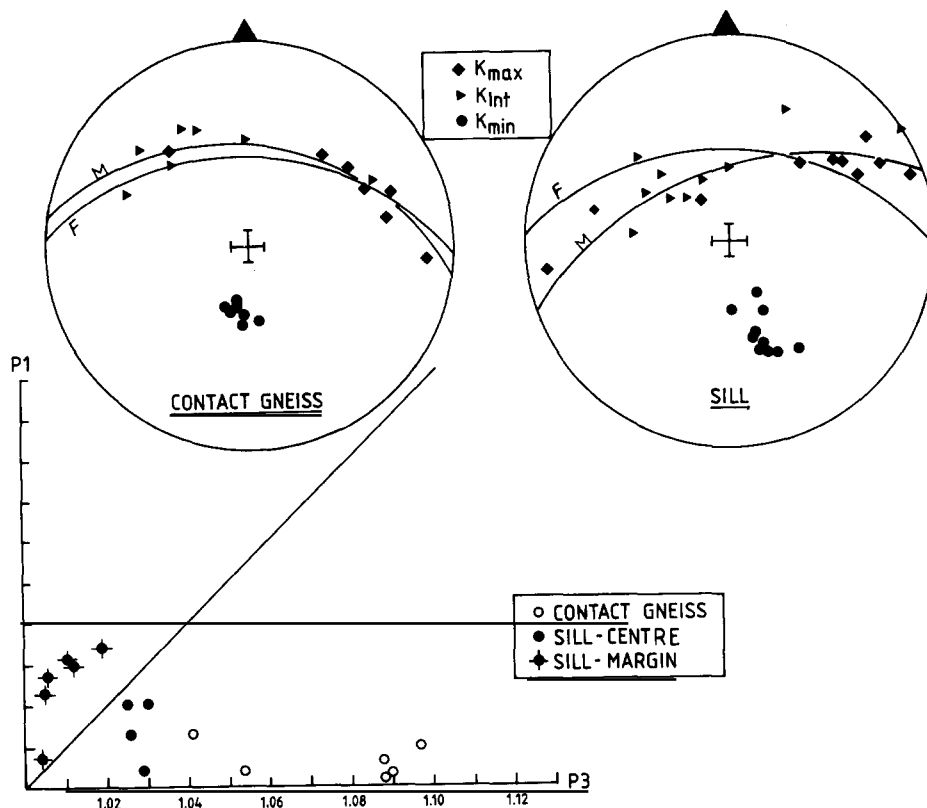


Fig. 3. Magnetic fabric data from the contact gneiss and the sill. In stereoplots, the principal axes are plotted as downward-pointing directions (positive), and great-circles denoted M and F denote the best fitted magnetic foliation plane and observed foliation (also orientation of sill margin), respectively. Note from the Flinn diagram that marginal samples from the sill (specimen 13–17 and 24) show prolate magnetic ellipsoids.

steeply upward pointing, remanences as compared with the central and lower parts of the sill (Fig. 4B). However, these remanence directions are associated with NRM intensities $< 0.3\text{--}0.4 \text{ mA m}^{-1}$ and thus proved unsuitable for demagnetization and component analysis.

As indicated from the NRM measurements (Fig. 4A,B), the tested specimens show two different remanence components (Fig. 4C): (1) a low blocking (LB) component with northerly declinations and steeply downward pointing inclinations, and (2) a high blocking (HB) component with southerly declinations and shallow upward-pointing inclinations (only observed in the sill). Specimens from the lower and central parts of the sill are dominated by the HB component with pronounced unblocking in the $400\text{--}600^\circ\text{C}$ range, though the principal unblocking (discrete) takes

place above $630\text{--}650^\circ\text{C}$ (cf. Figs. 6 and 7D). From some of the specimens (cf. see T18T in Fig. 6) it is possible to see that the HB component removed in the $400\text{--}600^\circ\text{C}$ range differs from that erased above $600\text{--}650^\circ\text{C}$. The directional differences are typically $< 5\text{--}10$ degrees of arc, and the highest HB component (HB_{II}) is somewhat shallower (see Fig. 4D and 6-T18T) than the component demagnetized in the $400(300)\text{--}600^\circ\text{C}$ range (HB_I). Thermomagnetic analysis and the thermal blocking spectra from specimens in the central and lower part of the sill (Fig. 7C,D) indicate the dominance of haematite with accessory magnetite. Secondary formation of magnetite is readily produced at temperatures above 600°C . AF demagnetization of these specimens (Fig. 7E) proved unsuitable due to dominance of the high coercivity haematite phase.

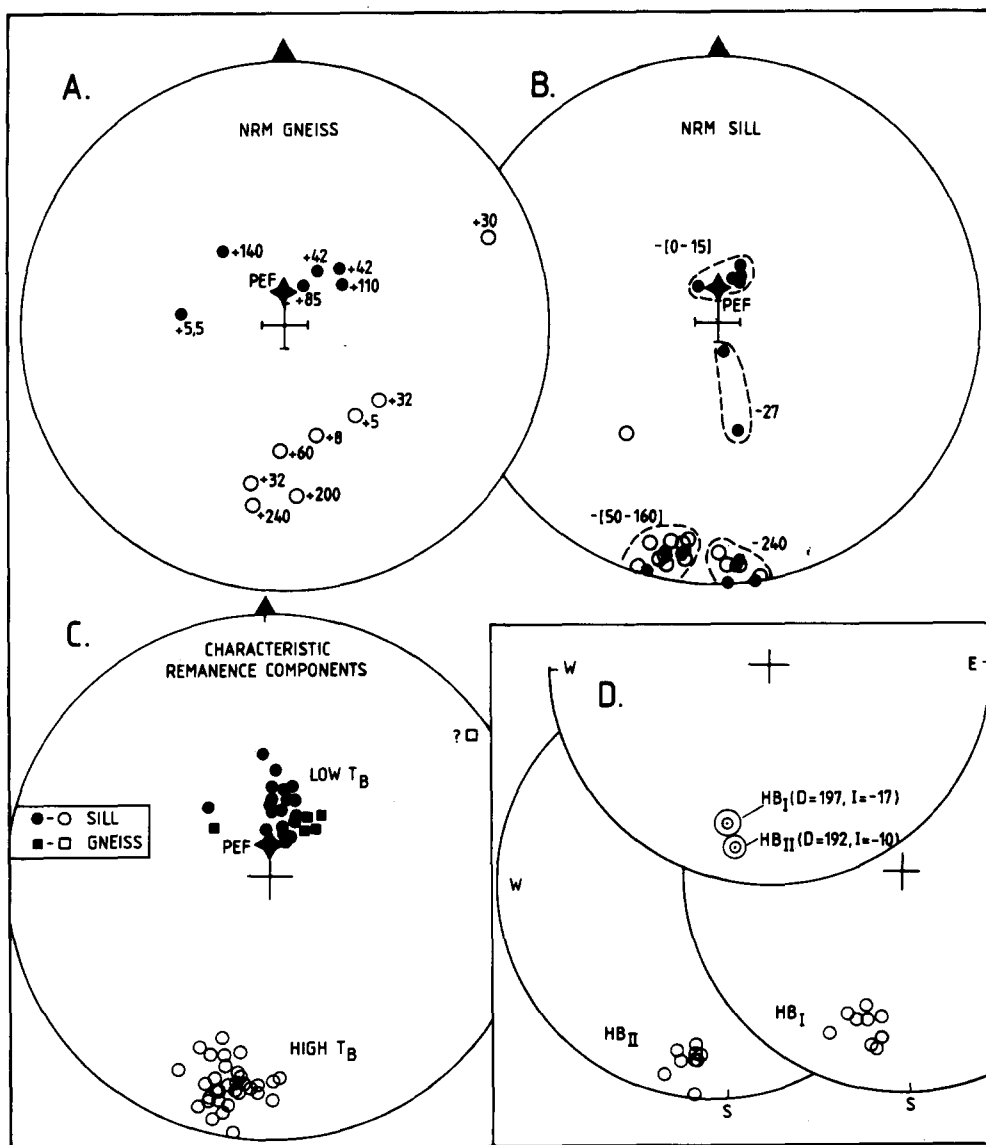


Fig. 4. Directional distribution of NRM from the gneiss (A) and the sill (B). (C) Characteristic remanence components after stability testing yielding one group of low blocking components (LB) and a southerly group of high-blocking components (HB) are shown. In some specimens it proved possible to separate the HB component into a 'magnetite' (HB_I) and 'haematite' (HB_{II}) component (D). Throughout this paper open (closed) symbols in the stereoplots defined upward (downward) pointing remanences. PEF = Present Earth Field. Numbers in (A) and (B) denote sampling position in centimetres above (+) and below (-) the upper sill contact (cf. Fig. 2).

In the lower and central parts of the sill, the HB component always shows some contamination of the LB component (Fig. 6; T18T), and the latter is typically randomized below 200–300 °C. The LB component is most likely resident in mag-

netite (see Fig. 7), whereas the HB component is carried by both magnetite and haematite. Passing upward toward the contact, the importance of the LB component increases (Fig. 6; T17B) and in the upper part of the sill the LB component totally

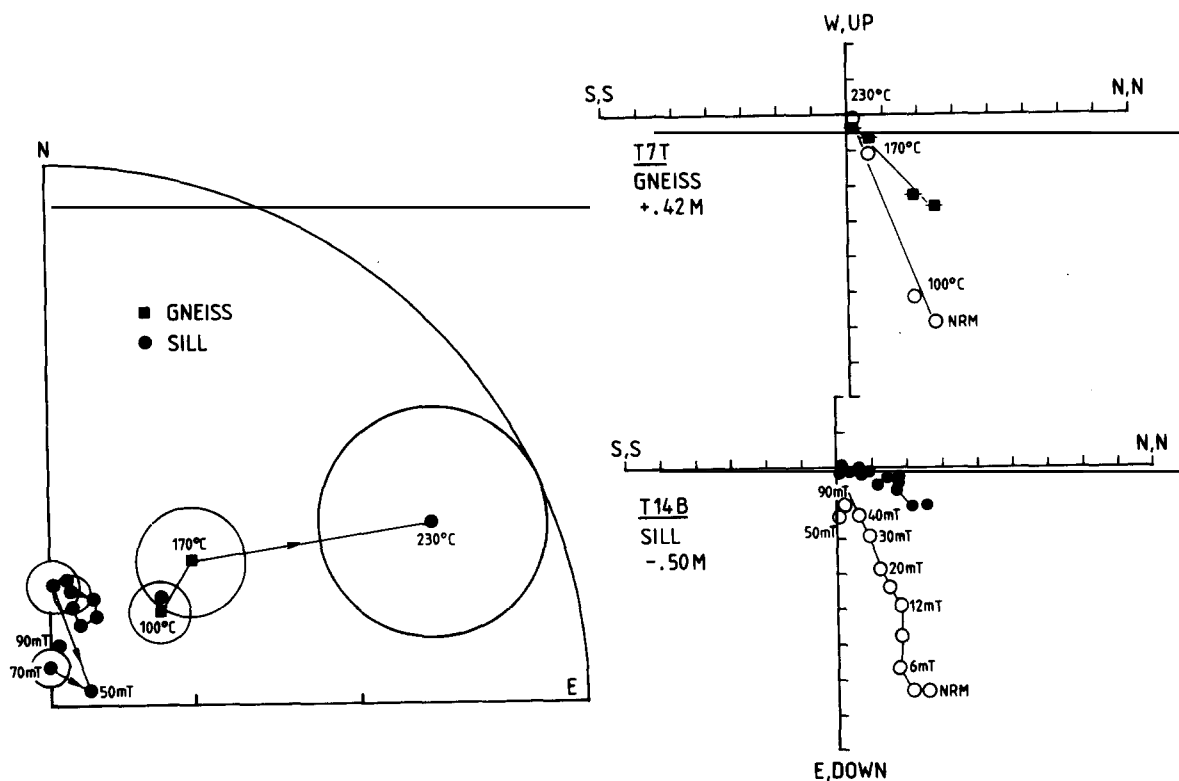


Fig. 5. Examples of thermal and AF demagnetization of a gneiss (T7T) and sill specimen (upper part of sill: T14B), respectively, which show the dominance of the LB component (cf. text). In orthogonal vector-projections open (closed) symbols represent points in the vertical (horizontal) plane. In stereoplots, the 95% confidence circle for each measurement during stepwise demagnetization is shown (if exceeding the size of the plotting symbol).

dominates the NRM (Fig. 5; T14B). From samples 13–15 the HB component was not identified, and these samples are characterized by major unblocking below 300 °C (cf. Fig. 7E) and medium destructive fields around 20 mT. As previously stated the NRM intensity in the contact gneiss is at

the limit of the instrumental noise level, and specimens subjected to thermal demagnetization show a poorly-defined remanence component similar to the LB component observed in the sill (see Figs. 4C and 5).

TABLE 1

Overall palaeomagnetic data

| Component | <i>D</i> | <i>I</i> | <i>N</i> | α_{95} | Pole | | dp/dm |
|----------------------------------|----------|----------|----------|---------------|------|-------|-------|
| | | | | | N | E | |
| LB component (Sill & Gneiss) | 008 | +61 | 26 | 4.5 | 68.2 | 172.3 | 5/7 |
| HB component (Sill) | 192 | −12 | 33 | 2.4 | 32.1 | 174.4 | 1/2 |
| (^a HB _I) | 196 | −17 | 9 | 4.4 | 34.2 | 169.3 | 2/5) |
| (HB _{II}) | 192 | −10 | 9 | 3.3 | 31.1 | 174.5 | 2/3) |

D is mean declination, *I* is mean inclination, *N* is number of specimen-directions, α_{95} = radius of 95% confidence circle (Fisher, 1953), dp, dm = semi-axis of the oval of 95% confidence about the mean pole.

^a Statistics on HB data where it proved possible to separate this into two components. (Sampling location: N63.3, E8.5).

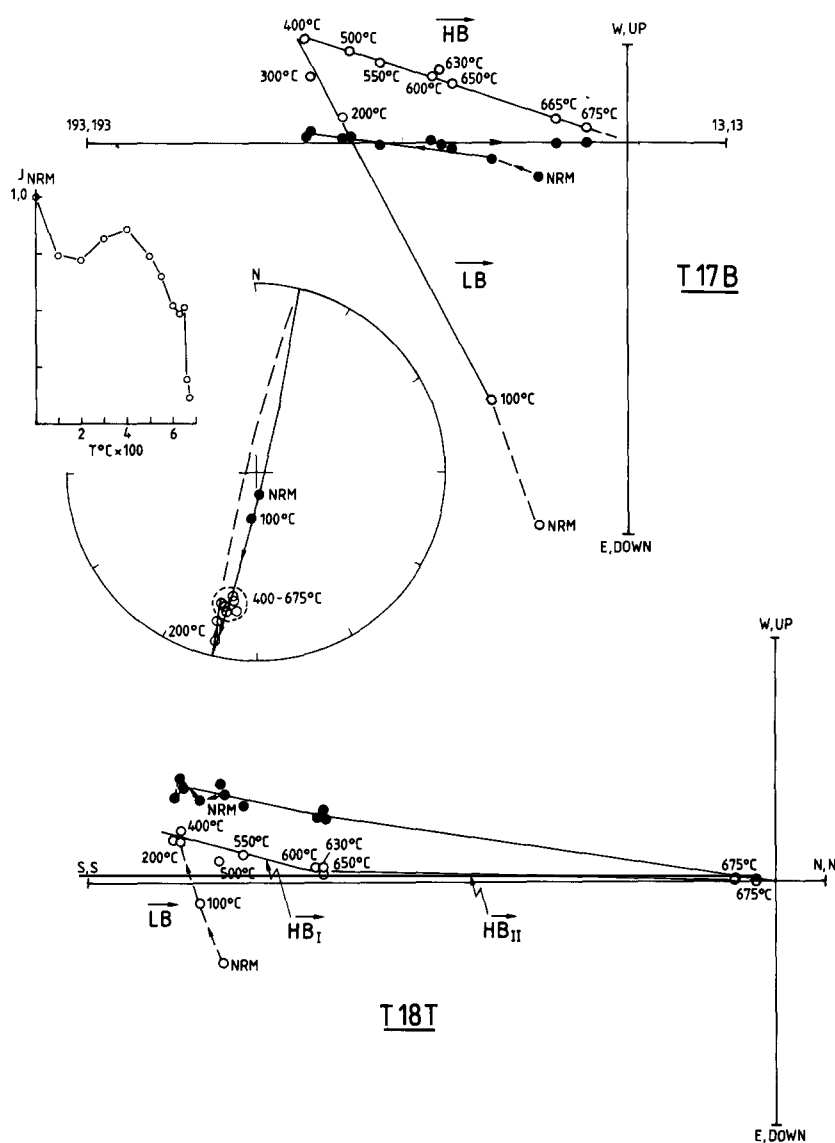


Fig. 6. Examples of thermal demagnetization of sill specimens. (cf. text). Conventions as Fig. 5. Stereoplot and decay curve refers to T17B. Note that T17B is optimal projected with respect to the HB component.

3. Discussion

Palaeomagnetic experiments show that the contact gneiss and notably the uppermost part of the sill are strongly contaminated by a secondary magnetization essentially carried by magnetite. We attribute this to a type of thermochemical overprinting (TCRM) facilitated by hydrothermal/fluid circulation along the contact. Locally, at the

contact a number of small faults with displacements in the order of only a few millimetres can be observed which may relate to this. The overall palaeomagnetic data (Table I) indicate a young origin, and most likely of Cretaceous or early Tertiary age. Faulting during this time is well documented from off-shore data (Gabrielsen, 1984).

The principal HB component, observed in the

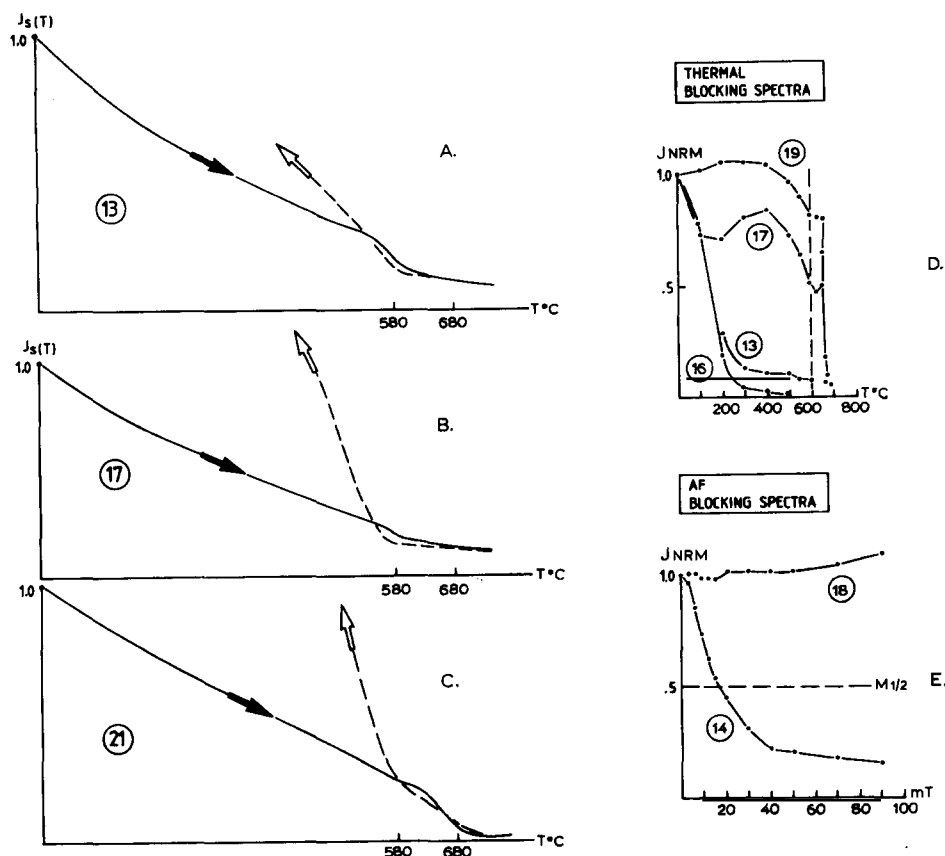


Fig. 7. Thermomagnetic analysis of a specimen from the upper part of the sill (A), a transitional specimen (B) and the central/lower part of the sill (C). Note the dominance of magnetite in AB (also notably affected by the LB component), whereas in (C) haematite almost totally dominate. Note that secondary production of magnetite is observed at all levels. (D) The variation in thermal blocking spectra from the upper part (13–16), the transition (17) and the central (lower) part (19) is shown. Note the increasing importance of haematite (i.e. blocking above 600 °C). In (e) the contrast in response to AF demagnetization is shown between an upper sill specimen (14) and the central part (18), the latter strongly dominated by high-coercivity mineral phases (haematite).

sill, is carried by both haematite (dominant) and magnetite. In a felsic syenite almost pure magnetite would be expected to be the primary opaque phase. In some instances, directional differences between the 'magnetite' and haematite HB components can be observed (c. 5 degrees of arc). We suggest that the magnetite is of primary origin and that it relates to the initial cooling of the sill and that the haematite was formed at an early stage of deuteric alteration. The directional differences (Table I), on the other hand, may reflect secular variation. As a result of the late magnetic overprint in the overlying gneiss and the uppermost part of the sill, it was not possible to obtain a

contact test with respect to the HB component. The pattern of NRM (Fig. 4A), however, clearly indicates that some of the gneissic specimens are influenced by a southerly component which may reflect the HB component, i.e. a contact magnetization (baked) relating to the intrusion of the sill.

Råheim (1974) drew attention to the geochemical similarity of the Tustna syenite and the Nordmarkite syenites of the Oslo rift. It is also of interest to note that the earliest rhomb-porphry lavas (Sundvollen, 1978), at Krogskogen, have been dated at 294 ± 5 (Rb/Sr; whole rock), i.e. virtually identical to Råheim's dating of the Tustna syenite. A lamprophyre dyke on the Island of

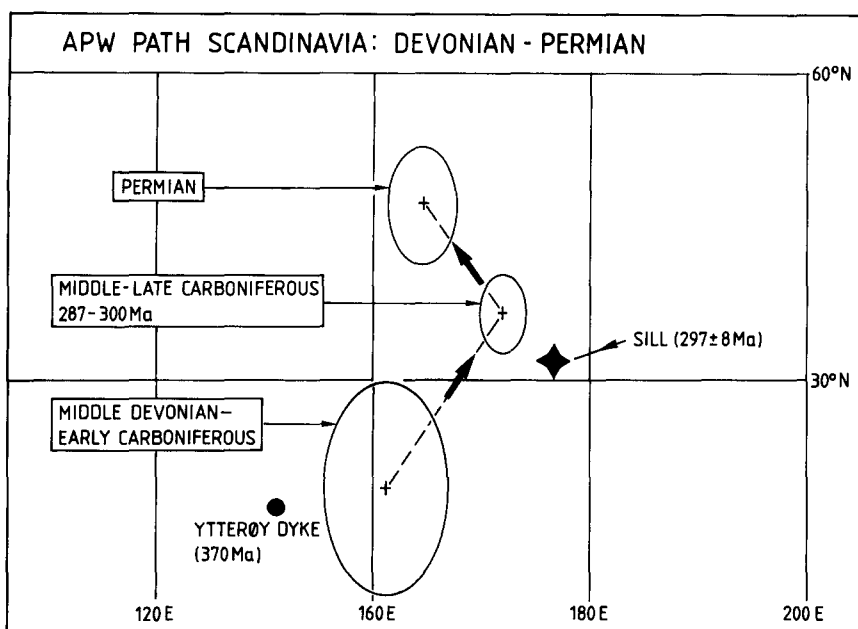


Fig. 8. Apparent Polar Wander path in the Devonian (mid-late) Permian range (from Pesonen et al., 1987) based on Scandinavian palaeomagnetic data (Galls Projection). Error confidences for the mean poles are 95% confidence circles (A95). The Stabben (present study) and Ytterøy (Storetvedt, 1967) poles are included in the diagram.

Ytterøy (north of Trondheim) has been the subject of discussion since Carstens (1961) suggested that the dyke was possibly related to Permian rifting. Palaeomagnetic data from the dyke (Storetvedt, 1967), however, clearly indicate an older age—probably Devonian (cf. Fig. 8). This latter has been subsequently confirmed by both K-Ar and $^{40}\text{Ar}/^{39}\text{Ar}$ dating of biotites at around 370 Ma (Priem et al., 1968; Mitchell and Roberts, 1986). It is, as yet, unclear whether this represents a primary magmatic age or reflects the cooling and uplift through the biotite blocking temperature.

In a recent compilation of all published palaeomagnetic data from Scandinavia (Pesonen et al., 1987) it has been possible to distinguish between Devonian (mid-late), Carboniferous (mid-late) and Permian palaeomagnetic poles. The mean poles shown in Fig. 8 were constructed on the basis of the Briden and Duff (1981) reliability classification (a-d quality poles), and the mean values only include a and b poles. Most palaeomagnetic poles from the Upper Carboniferous/Permian igneous rocks of the Oslo region (Douglass, 1987; summarized in Pesonen et al., 1987)

closely cluster around the established Permian pole. A consideration of the APW path (Fig. 8) shows that the relative pole-position for the HB component recorded in the Stabben sill is in reasonable correspondence with the mean Scandinavian Carboniferous pole (essentially based on Swedish rocks with radiometric ages in the 287–300 Ma range).

Although the Stabben pole may represent one of reliable Upper Carboniferous age in western Scandinavia, the authors would avoid use of the pole as a fixed point on the APW path at this stage. Firstly, the sampled unit may not represent a genuine time-average of the geomagnetic field, and secondly, the region contains many NE-SW trending faults of probably Mesozoic and post-Mesozoic age, and as yet it is not possible to propose what minor corrections should be made for fault-related tilting.

Acknowledgements

The Norwegian Research Council for the Humanities and Sciences (NAVF) and Falconbridge

A/S are thanked for financial support. Field assistance and discussions with Prof. D.M. Ramsay and H. Askvik are gratefully acknowledged. The figures were prepared in the drawing-office of the Norwegian Geological Survey. Norwegian Lithosphere Contribution (18).

References

- Askvik, H. and Rokoengen, K., 1985. Geologisk kart over Norge, berggrunnskart KRISTIANSUND-M. 1:250.000. Nor. Geol. Unders.
- Briden, J.C. and Duff, B.A., 1981. Pre-Carboniferous palaeomagnetism of Europe North of the Alpine Orogenic Belt. In: M.W. McElhinny and D.A. Valencio (Editors), *Palaeoreconstruction of the Continents*, Am. Geophys. Union, Geol. Soc. Am., pp. 137–149.
- Carstens, H., 1961. A post-Caledonian ultrabasic lamprophyre dyke on the Island Ytteroy in the Trondheimsfjord, Norway. *Geol. Fören. Stoch. Förh.*, 102: 403–420.
- Douglass, D.N., 1987. Palaeomagnetism of Ringerike Old Red Sandstone and related rocks, Southern Norway; implications for large separation of Baltica and British Terranes. *Tectonophysics*, submitted.
- Fisher, R.A., 1953. Dispersion on a sphere. *Proc. R. Soc. London Ser. A*, 217: 295–305.
- Gabrielsen, R.H., 1984. Long-lived fault zones and their influence on the tectonic development of the southwestern Barents Sea, J. Geol. Soc., 141: 651–662.
- Mitchell, J.G. and Roberts, D., 1986. Ages of lamprophyre dykes from Ytteroy and Lerkehaug, near Steinkjer, Central Norwegian Caledonides. *Nor. Geol. Tidsskr.*, 66: 255–262.
- Pesonen, L., Torsvik, T.H., Bylund, G. and Elming, S.Å., 1987. Crustal evolution of Fennoscandia—palaeomagnetic constraints. *Tectonophysics*, submitted.
- Priem, H.N.A., Verschure, R.H., Boelrijk, N.A.I.M., Hebeda, E.H. and Thorkildsen, C.D., 1968. Rb–Sr and K–Ar age measurements on phlogopitic biotite from the ultrabasic lamprophyre dyke on the Island of Ytteroy, Trondheimsfjord, Norway. *Nor. Geol. Tidsskr.*, 48: 319–321.
- Råheim, A., 1974. A post Caledonian Syenite porphyry dyke in the Western Gneiss region, Tustna, Central Norway. *Nor. Geol. Tidsskr.*, 54: 139–147.
- Storetvedt, K.M., 1967. Magnetic properties of an ultrabasic biotite lamprophyre dike from the Island of Ytteroy, Norway. *Nor. Geol. Tidsskr.*, 47, 2.
- Sundvoll, B., 1978. Isotope and trace-element chemistry, geochronology. In: J.A. Dons and B.T. Larsen (Editors) *The Oslo Palaeorift. A Review and Guide to Excursions*. NGU, 337: 35–40.